Effects of Crowding by Mono-, Di-, and Tetrasaccharides on Cytochrome *c*−Cytochrome *c* Peroxidase Binding: Comparing Experiment to Theory†

Artemiza S. Morar, Xuming Wang, and Gary J. Pielak*

Department of Chemistry, University of North Carolina at Chapel Hill, Chapel Hill, North Carolina 27599-3290

Received October 2, 2000; Revised Manuscript Received November 13, 2000

ABSTRACT: In cells, protein−protein interactions occur in an environment that is crowded with other molecules, but in vitro studies are almost exclusively performed in dilute solution. To gain information about the effects of crowding on protein complex formation, we used isothermal titration calorimetry to measure the stoichiometry, the free energy change, and the enthalpy change for the binding of yeast iso-1-ferricytochrome *c* to yeast ferricytochrome *c* peroxidase in dilute solution and in solutions crowded with the sugars glucose, sucrose, and stachyose. The stoichiometry is 1:1 under all conditions. The sugars stabilize the complex, but by only 0.1−0.5 kcal·mol^{-1}, and the increased stability is not correlated with the change in enthalpy of complex formation. We then compared the measured stability changes to values obtained from several analyses that are currently used to predict crowding-induced changes in biomolecular equilibria. None of the analyses are completely successful by themselves, and the results suggest that a complete analysis must account for both excluded-volume and chemical interactions.

Proteins have evolved to function within cells where macromolecule and small molecule solutes are present in high concentrations. These solutes can occupy >50% of the total cellular volume (*1*−*3*). However, nearly all in vitro studies are conducted in dilute solution where the volume occupied by macromolecules and other solutes is <1%. The term "molecular crowding" describes the effect of high solute concentrations on chemical reactions (*4*).

The volume occupied by solutes is unavailable to other molecules because two molecules cannot be in the same place at the same time. The thermodynamic consequences of the unavailable volume are called excluded-volume effects. It is important to remember that excluded-volume effects are present no matter what other interactions occur between the solution components (*4*). In addition to excluded-volume effects, solutes can interact chemically with other solution components. These interactions have been called soft interactions, binding interactions, and chemical interactions.

If excluded-volume effects are always present, why are they normally ignored? The answer is that protein chemists usually study tight binding in dilute solution. For example, excluded-volume effects can be ignored in dilute solution for the binding of oxygen to myoglobin, because the interaction is so tight that the total concentration of the ligand and receptor is too small to decrease the available volume. However, excluded volume cannot be ignored inside cells and in reactions where solutes affect protein equilibria only at high concentrations (e.g., sugars, urea, etc.).

It has been suggested that molecular crowding can have large effects on macromolecular equilibria, including protein−protein interactions (*5*), but few systematic studies are available. We have undertaken a systematic isothermal titration calorimetry study to probe the effects of sugar-induced crowding on the equilibrium thermodynamics for forming the structurally characterized (*6*) yeast iso-1-ferricytochrome *c* (Cc)[1]/yeast ferricytochrome *c* peroxidase (CcP) complex.

Several analyses have been developed in an effort to quantify the effects of high solute concentrations on the free energy of biological equilibria. Recently, we compared the results of protein denaturation studies conducted in the presence of sugars to analysis-based predictions and showed that both excluded-volume effects and cosolute binding are important for sugar-induced protein stabilization (*7, 8*). Here, we compare the results of protein complex formation studies conducted in the presence of sugars to the predictions of four analyses: osmotic-stress analysis (*9*), transfer-free-energy analysis (*10*), covolume analysis (*11, 12*), and a modified form of scaled-particle theory (*13, 14*).

MATERIALS AND METHODS

Proteins. Recombinant CcP was expressed and purified from *Escherichia coli* by using published protocols (*15, 16*). Crystals were stored in distilled−deionized water at −80 °C. The ratio of the absorbance at 408 nm to the absorbance at 280 nm was 1.2−1.3, showing that the CcP has a 5-coordinate high-spin heme (*17*). CcP concentrations were determined by using a molar absorptivity of 102 mM^{-1}·cm^{-1} at 408 nm (*17*). Recombinant yeast iso-1-Cc (*18*) was expressed and purified from *E. coli* by using a published protocol (*19*). Cc concentrations were determined at 410 nm by using a molar absorptivity of 106.1 mM^{-1}·cm^{-1} (*20*).

† This work was supported by NIH Grant GM42501.

* To whom correspondence should be addressed. Phone: (919) 966-3671. Fax: (919) 966-3675. E-mail: gary_pielak@email.unc.edu.

[1] Abbreviations: Cc, cytochrome *c*; CcP, cytochrome *c* peroxidase; DMG, dimethylglutaric acid; ITC, isothermal titration calorimetry.

10.1021/bi002296r CCC: $20.00
Published on Web 12/12/2000

ITC. Sugars were purchased from Sigma and used without further purification. Protein solutions were dialyzed (Slide-A-Lyzer membranes, 3500 and 7000 MWCO, Pierce) against 50 mM dimethylglutarate (DMG, Sigma), pH 6.0, with three buffer changes. The Cc and CcP solutions were dialyzed in the same beaker. The dialyzed proteins were filtered (0.2 μm) and degassed before use.

Titrations were performed with a Microcal MCS calorimeter. CcP (50−100 μM) was titrated with Cc (0.6−1.2 mM). The syringe was rotated at 200−400 rpm, the time between injections was 360−480 s, and the injection volume was 6−10 μL, but was constant for each experiment. Experiments were performed at 25 °C with an initial delay of 60 s and a reference offset of 30%. The reference cell contained distilled, deionized water. The external temperature bath was maintained at 20 °C.

Data were analyzed with Origin 5.0 (Microcal Software). Baseline and start and end points for integration were adjusted manually. Heats of dilutions were subtracted from the titration data before analysis. Data analysis requires a binding model with a set of fitting parameters. Given a model, the fitting program returns values for the binding constant, K, the binding enthalpy, $\Delta H^{\circ\prime\prime}$, and the stoichiometry (moles of Cc per mole of CcP), N. $\Delta H^{\circ\prime\prime}$ is the standard enthalpy of complex formation, where the standard state refers to 1 M reactants and products at 25 °C, 50 mM DMG, pH 6.0. $\Delta G^{\circ\prime\prime}$ was calculated from the equation $\Delta G^{\circ\prime\prime} = -RT \ln K$, and $-T\Delta S^{\circ\prime\prime}$ was calculated from $\Delta G^{\circ\prime\prime}$ and $\Delta H^{\circ\prime\prime}$ by using the equation $\Delta G^{\circ\prime\prime} = \Delta H^{\circ\prime\prime} - T\Delta S^{\circ\prime\prime}$ and standard techniques for error propagation (*21*). To obtain the fitted curves, iterations were performed until the fractional change in χ^2 was less than a tolerance value and χ^2 stopped decreasing. A χ^2 value of 3×10^3 indicates a good fit. The average χ^2 value for the present studies was 1.5×10^3 with a range of 7×10^2 to 3.1×10^3. Fitting uncertainties were always smaller than experimental uncertainties, suggesting that the data are well fit by the model and that the uncertainties reflect random errors.

Several observations suggest that a 1:1 complex is formed in dilute solution and in glucose, sucrose, and stachyose solutions. First, the shapes of the titration curves (Figure 1) are consistent with a 1:1 stoichiometry. Second, fitting to the one-set-of-sites model gave stoichiometries of between 0.87 and 1.15 (Table 1). Third, the data could not be fit to a 2:1 model. Given the protein concentrations used here, we could not detect a second binding site if $|\Delta H^{\circ\prime\prime}|$ is $\lesssim$1.0 kcal·mol^{-1}, or $\Delta G^{\circ\prime\prime}$ is $\gtrsim -2.0$ kcal·mol^{-1} (*16*, *22*).

Radii, Surface Areas, and Volumes. Sugar radii were estimated by using a bond counting approach (*23*). Solvent-accessible surface areas (SASAs) and solvent-accessible volumes were calculated by using the program GEPOL (*24*) with standard atomic radii (*16*) and a water radius of 1.4 Å. The SASAs and volumes for Cc (5918 Å^2, 22 181 Å^3), CcP (12 708 Å^2, 57 104 Å^3), and the complex (17 390 Å^2, 78 472 Å^3) were determined by using the coordinates from the crystal structure, 2PYCC (*6*). The radii of Cc (22 Å), CcP (31 Å), and the complex (37 Å) were calculated from their SASAs by assuming that each can be represented by an equivalent sphere.

Modified SPT. Berg's method (*14*) was modified to treat a heterodimer by using the equations given by Boublík (*13*). See Supporting Information for details.

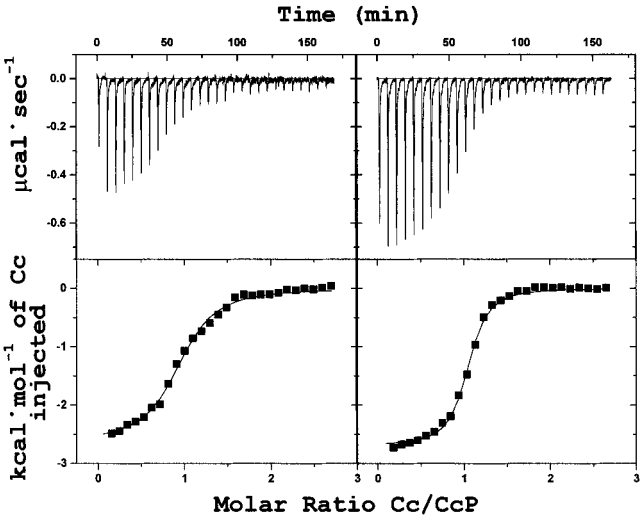

FIGURE 1: ITC data for the interaction between Cc and CcP at 25 °C, in 50 mM DMG, pH 6.0. The upper panels show the data after baseline correction. The lower panels show the integrated heats (■) and the best-fit curve (—) to a 1:1 binding model. The left-hand panels show data collected in dilute solution (1.06 mM Cc titrated into 53.5 μM CcP, 6 μL per injection). The right-hand panels show data collected in 2.5 M glucose (1.24 mM Cc into 81.2 μM CcP, 8 μL per injection).

RESULTS

We used ITC to study the thermodynamics for forming the Cc/CcP complex as a function of sugar size and sugar concentration. Representative data are shown in Figure 1, and the fitted parameters are presented in Table 1. $\Delta G^{\circ\prime\prime}$ and $\Delta H^{\circ\prime\prime}$ are presented in terms of complex formation. The data are of high quality, the results are consistent with 1:1 binding, and the data cannot be fit to a 2:1 model. The values for complex formation in dilute solution are different from those reported previously (*16*) because in the previous study we used authentic yeast iso-1-Cc and here we used the recombinant protein expressed in *E. coli*, which lacks the three methyl groups on lysine 72 (*18*, *19*).

The data in Table 1 show that sugar size and concentration have only a small ($\leq$0.5 kcal·mol^{-1}) stabilizing effect on $\Delta G^{\circ\prime\prime}$. Furthermore, there is no clear dependence of $\Delta G^{\circ\prime\prime}$ on sugar concentration, and sugars affect both $\Delta H^{\circ\prime\prime}$ and $\Delta S^{\circ\prime\prime}$. This stabilization is much weaker than for protein folding, where we observed values of up to 1.5 kcal·mol^{-1} under similar conditions (*7*, *8*). Nevertheless, our data on complex formation in the presence of high concentrations of small cosolutes are consistent with data from other studies (*25*−*27*).

DISCUSSION

Several analyses have been proposed to explain the effect of small-molecule crowding on biological equilibria. We set out to compare our results to four analyses that provide numerical predictions of sugar-induced changes in the free energy of complex formation: osmotic-stress analysis (*9*), transfer-free-energy analysis (*10*), covolume analysis (*11*), and a modified form of scaled-particle theory (*13*). The measured and predicted $\Delta\Delta G$ values are shown in Table 2.

Osmotic-stress analysis and transfer-free-energy analysis focus on soft interactions between solution components. Covolume analysis and scaled-particle theory focus on

Table 1: Thermodynamic Parameters for Forming the Cc/CcP Complex in Dilute Solution and in the Presence of a Monosaccharide, Disaccharide, and Tetrasaccharide[a]

sugar	[sugar], M	N	$\Delta H^{\circ\prime\prime}$	$-T\Delta S^{\circ\prime\prime}$	$\Delta G^{\circ\prime\prime}$
none	0	1.04 ± 0.15	-2.3 ± 0.4	-5.3 ± 0.5	-7.7 ± 0.1
glucose (monosaccharide)	0.50	1.03 ± 0.01	-2.5 ± 0.1	-5.3 ± 0.1	-7.8 ± 0.1
	1.5	1.15 ± 0.05	-2.0 ± 0.1	-5.8 ± 0.2	-7.8 ± 0.2
	2.5	1.06 ± 0.03	-2.6 ± 0.1	-5.6 ± 0.2	-8.2 ± 0.3
sucrose (disaccharide)	0.40	0.90 ± 0.05	-2.5 ± 0.2	-5.6 ± 0.1	-8.1 ± 0.2
	1.2	0.87	-2.9	-5.2	-8.1
stachyose (tetrasaccharide)	0.30	0.96 ± 0.01	-2.9 ± 0.2	-5.1 ± 0.2	-8.0 ± 0.3

[a] The stoichiometry, N, is the ratio of Cc to CcP. $\Delta H^{\circ\prime\prime}$, $-T\Delta S^{\circ\prime\prime}$, and $\Delta G^{\circ\prime\prime}$ are in kcal·mol^{-1}. Experiments were performed at pH 6.0, 25 °C, in 50 mM DMG. Values for experiments performed in glucose, stachyose, and 0.4 M sucrose are the average and standard deviation from three titrations. Values for experiments performed in 1.2 M sucrose are the average of two titrations.

Table 2: Observed and Calculated Changes in the Free Energy of Complex Formation[a]

sugar radius, Å	[sugar], M	$\Delta\Delta G^{\circ\prime\prime}$, kcal·mol^{-1}, obsd	$\Delta\Delta G$, kcal·mol^{-1}, calc					
			transfer free energy	covolume	scaled-particle theory, $L =$ 1.000	0.875	0.833	0.810
glucose 3.2	0.50	-0.1 ± 0.1	nd	-0.2	0.5	0.1	0.0	-0.1
	1.5	-0.1 ± 0.2	nd	-0.5	1.6	0.3	-0.1	-0.3
	2.5	-0.5 ± 0.3	nd	-0.9	2.9	0.6	-0.2	-0.6
sucrose 4.0	0.40	-0.4 ± 0.2	-1.5	-0.2	0.7	0.2	0.0	0.0
	1.2	-0.4	-6.3	-0.5	3.5	0.9	0.0	-0.4
stachyose 5.0	0.30	-0.3 ± 0.3	nd	-0.2	0.9	0.3	0.1	0.0

[a] $\Delta\Delta G^{\circ\prime\prime}$ was calculated from the data in Table 1. A negative $\Delta\Delta G$ indicates that the complex is stabilized relative to dilute solution. nd, not determined because model compound transfer free energies have not been reported.

excluded volume. The interactions involved in excluded-volume-based analyses are called hard interactions because the molecules are treated as hard objects. That is, the interaction energy between the particles is zero if the two particles do not touch, and increases to infinity if the hard bodies try to interpenetrate each other. Because only hard interactions are considered, these analyses focus on the entropy of complex formation. A first indication that excluded-volume-based analyses do not provide a complete explanation comes from the fact that sugars affect both $\Delta S^{\circ\prime\prime}$ and $\Delta H^{\circ\prime\prime}$ (Table 1).

Binding-Based Analyses

Osmotic Stress. This analysis attempts to explain the effect of cosolutes on complex stability by considering cosolute-induced changes in water activity, which can be related to water binding. According to this analysis, cosolutes will stabilize complexes if water is released upon complex formation and destabilize complexes if water is taken up. Osmotic-stress analysis has been criticized on thermodynamic grounds (*28*, *29*), but we discuss it here because it is widely applied (*30*).

The $\Delta\Delta G^{\circ\prime\prime}$ values in Table 2 show that cosolute size and concentration have only a small stabilizing effect on complex formation. In terms of osmotic-stress analysis, this means that there is no net water release or uptake upon complex formation. Thermodynamic criticisms notwithstanding, this conclusion is inconsistent with the observations that while the individual proteins are solvated, the crystal structure of the complex shows no room for water at the protein−protein interface (*6*).

Transfer Free Energies. The effects of cosolutes on complex stability have also been interpreted in terms of differences in the free energy required to transfer the reactants and products from dilute solution to a concentrated cosolute solution (*10*, *31*, *32*). Model compound data are used to determine the transfer free energies for the protein backbone and the amino acid side chains. This analysis has been applied to protein folding as follows. First, the SASA of backbone and side chains that are buried upon folding is determined. Second, the buried SASAs for each moiety (i.e., the 19 side chains and the backbone) are summed and scaled to the standard SASA of the moiety (*33*) to determine the number of each moiety that is buried upon folding. Third, this number is multiplied by the appropriate model transfer free energy, and transfer free energies are summed to give the predicted change in stability.

One potential difficulty is that the model transfer free energies are based on concentrations, not activities. That is, the transfer free energies are calculated from water and sucrose solubilities by assuming that the activity coefficients of the amino acids are the same in water and sucrose solution. With the exception of tryptophan, phenylalanine, tyrosine, and histidine, the amino acid and backbone transfer free energies are less than $\sim|50|$ cal·mol^{-1} (*10*). For such small values, a 10% change in activity coefficient could reverse the sign of the transfer free energies, and even a 5% difference can change the conclusions. For several solutions, there is more amino acid (by weight) than water, so a 5% difference may be conservative. Nevertheless, transfer-free-energy analysis has proven useful in explaining the protein-stabilizing effect of solutes (*10*, *31*, *32*, *34*, *35*).

For studies of protein stability, another potential difficulty is that the surface areas of the denatured states must be estimated. This difficulty does not apply to structurally characterized protein complexes. Assuming that the structure

of the reactants does not change on complex formation, the surface areas of the reactants and products can be calculated from the crystal structure coordinates of the complex. This assumption is true for the Cc/CcP complex (*6*).

We applied transfer-free-energy analysis to the formation of the Cc/CcP complex in sucrose, because this is the only sugar for which transfer free energies have been reported (*10*). The model compound transfer free energies were measured in 0.5 and 1.0 M sucrose. We corrected the values to 0.4 and 1.2 M sucrose by multiplying the reported values by 0.80 and 1.2, respectively. The expected change in binding free energy on going from water to sucrose was calculated as described above for protein stability except that all the SASAs were calculated from the crystal structure coordinates of the individual proteins and the complex.

The results are shown in Table 2. Transfer-free-energy analysis overestimates the observed $\Delta\Delta G^{\circ\prime\prime}$ by a factor of between about 4 and 15. The calculations must be considered approximate because of the simplistic method used to correct the model compound data, but it seems unlikely that the correction explains all of the difference. Another reason for the discrepancy may be that transfer-free-energy analysis does not completely account for excluded volume.

Excluded-Volume-Based Analyses

In these analyses, the components are treated as hard spheres. An obvious shortcoming is that soft interactions are ignored. In applying these analyses, we assume that there is no protein concentration dependence. This assumption is reasonable because the protein concentrations (<100 μM) are much less than the cosolute concentrations (M).

Covolume Analysis. The covolume, *U*, is the volume of a sphere whose radius is the sum of the protein and cosolute radii (*12*, *36*). The excluded volume depends on the sizes of the protein and the cosolute and on the cosolute concentration. At a fixed cosolute concentration, excluded-volume effects will drive a reaction toward products if the covolume of the products is less than the covolume of the reactants.

An advantage of the excluded-volume theory is that the covolume, *U*, can be directly associated with a fundamental thermodynamic parameter, specifically that part of the second virial coefficient due to hard interactions between the protein and the sugar (*12*):

$$U = \frac{3}{4}\pi N(r_2 + r_3)^3$$

where N is Avogadro's number, r_2 is the radius of the protein, and r_3 is the radius of the sugar.

For protein complex formation, the change in the binding free energy at a fixed sugar concentration (C_3) is calculated by using the equation (*11*):

$$\Delta\Delta G = -RT[U_{\mathrm{Cc/CcP}} - (U_{\mathrm{Cc}} + U_{\mathrm{CcP}})]C_3$$

where R is the gas constant, T is the absolute temperature, and U_X refers to the covolume of the individual proteins and the complex.

The results are shown in Table 2. The predicted stabilization is larger than the observed stabilization, but the agreement is quite good considering the simplicity of the theory and the large number of assumptions and approximations. Taken at face value, the mismatch between the observed and calculated values suggests that soft interactions destabilize the complex, a conclusion inconsistent with the stabilization predicted by transfer-free-energy analysis.

Covolume analysis assumes that complex formation does not result in a shape change. That is, the complex is treated as a sphere whose volume is simply the sum of the volume of the two spherical proteins. Next, we consider an analysis that allows a change in shape.

Scaled-Particle Theory. Scaled-particle theory gives the free energy for forming a cavity in the solution that is large enough to contain the protein (*37*). Unlike excluded-volume theory, which treats only the cosolute and the protein, the version of scaled-particle theory used here (*14*) also considers the solvent.

A potential advantage of the theory used here is that the shape of the products and reactants can be different (*13*). Specifically, Cc and CcP can be treated as spheres of different size, and the complex can be treated as a heterodimer of kissing spheres. Furthermore, the calculations can be performed as a function of the distance between the centers of the kissing spheres (*13*). This parameter, *L*, is the ratio of the distance between the centers to the sum of their radii. A value of unity indicates kissing spheres whose total volume equals the sum of the individual volumes. Intermediate values indicate partial penetration of one sphere into another with a concomitant volume reduction, and a value of 0 indicates that the smaller sphere lies completely within the larger sphere. It is important to note that the complex is still a hard object; the volume reduction only changes its shape.

Scaled-particle theory suffers from some of the same potential problems as excluded-volume theory: soft interactions are ignored, and all the components are treated as spheres. The ability of scaled-particle theory to treat water explicitly is an additional potential disadvantage because it adds another adjustable parameter and because the results are not strictly comparable to an authentic thermodynamic parameter (*38*).

The expected change in complex stability on going from dilute solution to sugar solution is calculated in four steps. First, the free energy of cavity formation is calculated for each species (Cc, CcP, and the complex) in dilute solution. Details of the calculations are given in the Supporting Information and in the original references (*7*, *8*, *13*, *14*). Second, the sum of the energies for Cc and CcP is subtracted from the energy for the complex to give the relative free energy for complex formation in dilute solution. Third, the first two steps are repeated for the sugar solution. Fourth, the relative free energy for complex formation in dilute solution is subtracted from the relative free energy of complex formation in sugar solution to give the expected change in complex stability.

The results are shown in Table 2. When $L = 1$ (i.e., no volume reduction upon complex formation), the analysis predicts that sugars will destabilize the complex. This result is most easily rationalized in terms of cavity location: it is more probable that two cavities will form anywhere in solution than next to each other (*14*). However, the calculated and observed values have opposite signs. Taking the calculated result at face value, the opposite signs mean that soft interactions stabilize the complex. This scenario is in

accord with the results from transfer-free-energy analysis. Nevertheless, it is unwise to place too much confidence in the above speculation because the assumption of no volume change is not strictly valid. The solvent-accessible volume of the complex is 1.03% less than the sum of the volumes for uncomplexed Cc and CcP. This volume decrease corresponds to an L value of 0.875. As shown in Table 2, using this value brings the calculated and observed results into closer agreement. Using a value of 0.833, which corresponds to a volume reduction of 2.25%, gives the best agreement. These results suggest that soft interactions may be unimportant.

Summary. We have shown that high concentrations of mono-, di-, and tetrasaccharides have a small stabilizing effect on formation of the 1:1 Cc/CcP complex. This observation is in accord with the results of other studies (*25*−*27*). Recently, we showed that sugars have a much larger effect on protein stability (*7, 8*). The disparity between these two results is probably due to the fact that more surface area is buried per gram of protein when a denatured protein folds than when two folded proteins bind.

We compared our results on complex formation to analyses based on binding and excluded-volume effects, but none of the analyses were completely satisfying. The results do not seem to be compatible with osmotic-stress analysis because it suggests no change in solvation upon complex formation, and transfer-free-energy analysis overestimates the stabilizing effect. However, these analyses ignore excluded-volume effects. Covolume analysis predicts that sugars will stabilize the complex, while scaled-particle theory predicts stabilization or destabilization, depending on the volume reduction upon complex formation. However, these analyses ignore soft interactions.

The assumptions and approximations involved in the analyses make quantitative comparisons difficult, but our study highlights the challenges faced by those seeking a unified view of crowding-induced changes in protein complex stability. Comparisons of the results from scaled-particle theory and transfer-free-energy analysis to the measured $\Delta\Delta G^{\circ\prime\prime}$ values suggest that hard and soft interactions partially cancel each other. If this cancellation is real, then small-molecule crowding may have only a small effect on protein−protein binding when binding is not accompanied by a change in structure.

ACKNOWLEDGMENT

We thank Dorothy Erie, Aleister Saunders, and Paula Davis-Searles for inspiring these studies, Tom Poulos for providing the CcP expression system, Grant Mauk for providing the original version of the Cc expression system, and the Pielak group for helpful discussions.

SUPPORTING INFORMATION AVAILABLE

Details of the equations used for scaled-particle-theory calculations are provided (3 pages). This material is available free of charge via the Internet at http://pubs.acs.org.

REFERENCES

1. Capp, M. W., Cayley, D. S., Zhang, W., Guttman, H. J., Melcher, S. E., Saecker, R. M., Anderson, C. F., and Record, M. T., Jr. (1996) *J. Mol. Biol. 258*, 25−36.
2. Fulton, A. B. (1982) *Cell 30*, 345−347.
3. Yancey, P. H., Clark, M. E., Hand, S. C., Bowlus, R. D., and Somero, G. N. (1982) *Science 217*, 1214−1222.
4. Minton, A. P. (1997) *Curr. Opin. Biotechnol. 8*, 65−69.
5. Minton, A. P. (2000) *Curr. Opin. Struct. Biol. 10*, 34−39.
6. Pelletier, H., and Kraut, J. (1992) *Science 258*, 1748−1755.
7. Saunders, A. J., Davis-Searles, P. R., Allen, D. L., Pielak, G. J., and Erie, D. A. (2000) *Biopolymers 53*, 293−307.
8. Davis-Searles, P. R., Morar, A. S., Saunders, A. J., Erie, D. A., and Pielak, G. J. (1998) *Biochemistry 37*, 17048−17053.
9. Parsegian, V. A., Rand, R. P., and Rau, D. C. (2000) *Proc. Natl. Acad. Sci. U.S.A. 97*, 3987−3992.
10. Liu, Y., and Bolen, D. W. (1995) *Biochemistry 34*, 12884−12891.
11. Shearwin, K. E., and Winzor, D. J. (1988) *Biophys. Chem. 31*, 287−294.
12. Winzor, D. J., and Wills, P. R. (1995) in *Protein−Solvent Interactions* (Gregory, R. B., Ed.) pp 483−520, Marcel Dekker, New York.
13. Boublík, T. (1986) *Mol. Phys. 59*, 775−793.
14. Berg, O. (1990) *Biopolymers 30*, 1027−1037.
15. Fishel, L. A., Villafranca, J. E., Mauro, M., and Kraut, J. (1987) *Biochemistry 26*, 351−360.
16. Wang, X., and Pielak, G. J. (1999) *Biochemistry 38*, 16876−16881.
17. Dasgupta, S., Rousseau, D. L., Anni, H., and Yonetani, T. (1989) *J. Biol. Chem. 264*, 654−662.
18. Pollock, W. B., Rosell, F. I., Twitchett, M. B., Dumont, M. E., and Mauk, A. G. (1998) *Biochemistry 37*, 6124−6131.
19. Morar, A. S., Kakouras, D., Young, G. B., Boyd, J., and Pielak, G. J. (1999) *J. Biol. Inorg. Chem. 4*, 220−222.
20. Margoliash, E., and Frohwirt, N. (1959) *Biochem. J. 71*, 570−572.
21. Taylor, J. R. (1982) *An Introduction to Error Analysis*, University Science Books, Mill Valley, CA.
22. Pielak, G. J., and Wang, X. (2001) *Biochemistry* (in press).
23. Edward, J. T. (1970) *J. Chem. Educ. 47*, 261−270.
24. Silla, E., Tuñón, I., and Pascual-Ahuir, J. L. (1991) *J. Comput. Chem. 12*, 1077−1088.
25. Xavier, K. A., Shick, K. A., Smith-Gill, S. J., and Wilson, R. C. (1997) *Biophys. J. 73*, 2116−2125.
26. Reid, C., and Rand, R. P. (1997) *Biophys. J. 72*, 1022−1030.
27. Kornblatt, J. A., Kornblatt, M. J., Hoa, G. H., and Mauk, A. G. (1993) *Biophys. J. 65*, 1059−1065.
28. Timasheff, S. N. (1998) *Proc. Natl. Acad. Sci. U.S.A. 95*, 7363−7367.
29. Jacobsen, M. P., Wills, P. R., and Winzor, D. J. (1996) *Biochemistry 35*, 13173−13179.
30. Parsegian, V. A., Rand, R. P., and Rau, D. C. (1995) *Methods Enzymol. 259*, 43−94.
31. Baskakov, I., and Bolen, D. W. (1998) *J. Biol. Chem. 273*, 4831−4834.
32. Qu, Y., Bolen, C. L., and Bolen, D. W. (1998) *Proc. Natl. Acad. Sci. U.S.A. 95*, 9268−9273.
33. Lesser, G. J., and Rose, G. D. (1990) *Proteins: Struct., Funct., Genet. 8*, 6−13.
34. Wang, A., Robertson, A. D., and Bolen, D. W. (1995) *Biochemistry 34*, 15096−15104.
35. Santoro, M. M., Liu, Y., Khan, S. M., Hou, L. X., and Bolen, D. W. (1992) *Biochemistry 31*, 5278−5283.
36. Schachman, H. K., and Lauffer, M. A. (1949) *J. Am. Chem. Soc. 71*, 536−541.
37. Reiss, H. (1966) *Adv. Chem. Phys. 9*, 1−84.
38. Tang, K. E. S., and Bloomfield, V. A. (2000) *Biophys. J. 79*, 2222−2234.

BI002296R